Classical and Quantum Gravity

PURPOSE-LED PUBLISHING™

ACCEPTED MANUSCRIPT • OPEN ACCESS

Estimation of an upper limit on ground tilt noise in an underground research infrastructure as a benchmark for the Einstein Telescope

To cite this article before publication: Luca Naticchioni *et al* 2026 *Class. Quantum Grav.* in press https://doi.org/10.1088/1361-6382/aec109

Manuscript version: Accepted Manuscript

Accepted Manuscript is "the version of the article accepted for publication including all changes made as a result of the peer review process, and which may also include the addition to the article by IOP Publishing of a header, an article ID, a cover sheet and/or an 'Accepted Manuscript' watermark, but excluding any other editing, typesetting or other changes made by IOP Publishing and/or its licensors"

This Accepted Manuscript is **© 2026 The Author(s). Published by IOP Publishing Ltd**.



As the Version of Record of this article is going to be / has been published on a gold open access basis under a CC BY 4.0 licence, this Accepted Manuscript is available for reuse under a CC BY 4.0 licence immediately.

Everyone is permitted to use all or part of the original content in this article, provided that they adhere to all the terms of the licence https://creativecommons.org/licences/by/4.0

Although reasonable endeavours have been taken to obtain all necessary permissions from third parties to include their copyrighted content within this article, their full citation and copyright line may not be present in this Accepted Manuscript version. Before using any content from this article, please refer to the Version of Record on IOPscience once published for full citation and copyright details, as permissions may be required. All third party content is fully copyright protected and is not published on a gold open access basis under a CC BY licence, unless that is specifically stated in the figure caption in the Version of Record.

View the article online for updates and enhancements.

This content was downloaded from IP address 192.167.204.120 on 13/11/2026 at 08:19

Journal Name

Crossmark

RECEIVED
dd Month yyyy

REVISED
dd Month yyyy

PAPER

Estimation of an upper limit on ground tilt noise in an underground research infrastructure as a benchmark for the Einstein Telescope

L Naticchioni[1,2], L Trozzo[3], E Majorana[1,4], S Pirro[5], M Ricci[1,4], M Di Giovanni[6,7], S Miyoki[8], T Yokozawa[8], T Washimi[9]

[1]INFN - Sezione di Roma, I-00185 Roma, Italy [2]INGV - Sezione di Pisa, I-56125 Pisa, Italy [3]INFN - Sezione di Napoli, I-80126 Napoli, Italy [4]Sapienza - Università di Roma, Dipartimento di Fisica, I-00185 Roma, Italy [5]INFN - Laboratori Nazionali del Gran Sasso, I-67100 Assergi (AQ), Italy [6]Scuola Normale Superiore, I-56126 Pisa, Italy [7]INFN - Sezione di Pisa, I-56127 Pisa, Italy [8]University of Tokyo - Institute for Cosmic Ray Research, Kashiwa, Chiba 277-8582, Japan [9]National Astronomical Observatory of Japan, Mitaka, Tokyo 181-8588, Japan

E-mail: luca.naticchioni@roma1.infn.it

Keywords: seismic noise, tilt noise, gravitational wave detectors, Einstein Telescope, LNGS, KAGRA

Abstract

In this work, we present the results of an investigation into low-frequency seismic noise in an underground laboratory infrastructure, serving as a case study for the future Einstein Telescope. Specifically, we focus on the low-frequency noise measured at the Gran Sasso National Laboratory (*Laboratori Nazionali del Gran Sasso*, LNGS), expanding upon previous findings at the same location. Finally, we estimate upper limits on the expected tilt noise, considering only the ground contribution (i.e., without considering any other contributions from specific experimental setup), for frequencies below 70 mHz, using seismic data from LNGS and KAGRA. Finally, these underground upper bounds are superimposed and compared directly with the official active seismic isolation requirements of the Einstein Telescope. Our findings confirm that the ambient underground tilt levels comply with ET suspension control targets, providing vital engineering guidance for active tilt-attenuation strategies in next-generation gravitational-wave observatories.

1 Introduction

Einstein Telescope (ET) [1] underground interferometric detectors will require extremely stable and low seismic noise levels, particularly in the low-frequency band (i.e., below 20 Hz), to meet the observatory's sensitivity targets. Although the ET observation band officially starts at $2-3$ Hz [2], a significant excess of noise below this range can critically compromise the ET interferometer control. Specifically, low-frequency seismic disturbances couple directly into the complex suspension systems and active isolation controls (such as the Superattenuators [3]), generating control forces that can inject electronic noise or saturate the actuators, thereby degrading the detector's duty cycle and overall sensitivity.

The microseismic peaks [4, 5], produced by the interaction between ocean waves and the seafloor, are a well-known spectral feature observed globally on the Earth's surface, typically within the 50 mHz–300 mHz range. Higher-frequency microseismic peaks are also generated in semi-enclosed seas (e.g., the Mediterranean Sea), occurring between the oceanic microseismic peaks and approximately 1 Hz. At frequencies lower than the microseismic band, the seismic background generally exhibits a $1/f$-like trend, as described by Peterson's New Low Noise Model (NLNM) [7].

In this very-low frequency range, standard inertial sensors cannot distinguish between true horizontal translational acceleration and ground tilt, a fundamental limitation known as the tilt-translation coupling phenomenon. This constraint significantly affects horizontal seismic records at frequencies below 10 mHz [6]. Consequently, a significant increase in the horizontal channels below the microseismic band could be interpreted as an excess of environmental tilt noise, although discriminating between proper seismic acceleration, ground rotation, and other sensor-related effects (e.g., thermal convection or instrumental self-noise) is not straightforward.

Accepted Manuscript

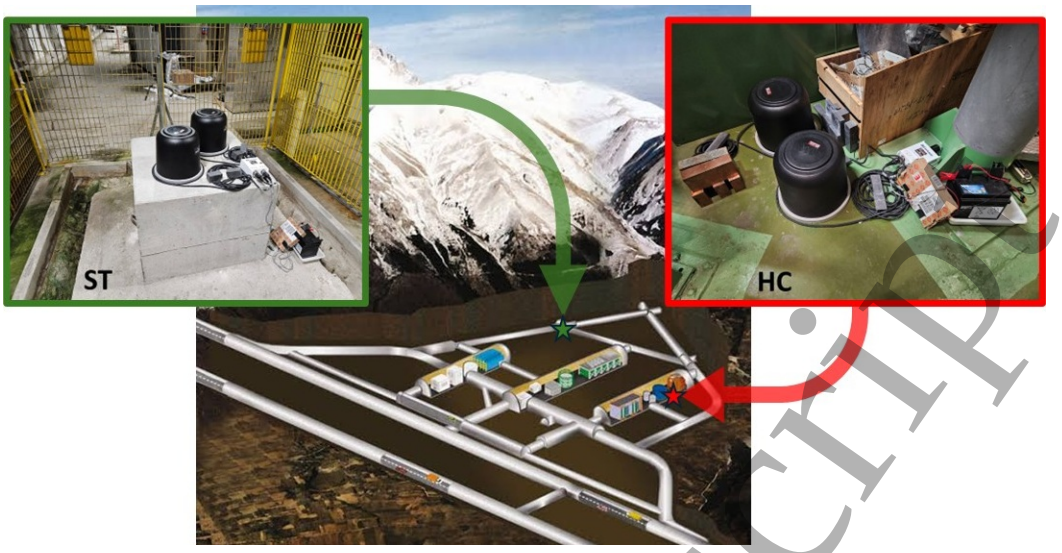


Figure 1: Scheme of the underground LNGS laboratory. The two arrows indicate the measurement locations (ST: service tunnel, HC: Hall C) where the pair of seismometers was installed during the survey.

Unlike other measurements of seismic background carried out in quiet underground environments (such as at the Sos Enattos candidate site in Sardinia [8, 9, 10, 11, 12]), earlier seismic noise measurements at the National Underground Laboratory of Gran Sasso (LNGS) reported a very high and significant excess below 70 mHz [13, 14], raising the urgent question of whether this could indicate a severe, site-dependent tilt noise induced within a large underground research facility. It should be noted, however, that the exact details of earlier measurements (such as those reported in [13]) remain partially unclear, including whether the seismometers were adequately shielded against environmental ventilation and localized convection currents. Proper sensor installation and thermal insulation are essential to obtain reliable, uncorrupted information about the true seismic noise floor in underground environments. Moreover, strong transients (e.g., major teleseismic events) are known to produce persistently elevated noise levels at low frequencies and must be strictly filtered and removed from the background analysis.

To provide a definitive and quantitative assessment of the low-frequency seismic background at LNGS, we installed two identical broadband (360 s period) seismometers in two different strategic locations: a service tunnel and the large experimental Hall C of the facility (respectively, ST and HC in Figure 1). The first point is inherently quieter than the second, as it is located in a service tunnel far from any experimental apparatus, while the second is in the experimental hall floor, near the location of the Borexino experiment [15]. The seismometers were placed approximately 40 cm apart and properly shielded from air flows and convective fluctuations. Under these controlled conditions, we aimed to evaluate the real noise level below the microseismic band and investigate the coherence function between the twin sensors, assuming that a genuine macroscopic ground tilt would produce a highly coherent signal between the two adjacent seismometers, although in that case it could not be clearly distinguished from a horizontal acceleration component experienced by the sensors.

In this work, we present the results of this rigorous investigation, providing a comparative case study for the future Einstein Telescope. By applying an extrapolation methology derived from Rodgers's work [16] to the seismic data from both LNGS and KAGRA, we derive conservative quantitative upper limits on the expected ground-induced tilt noise. These limits, filtered through a seismic isolation system, are then compared against the ET sensitivity curve to benchmark the feasibility of managing underground ambient tilt noise within current gravitational-wave detector suspension designs.

2 Seismic noise at LNGS

2.1 Sensors Installation

The first measurement location was the crossing point between two service tunnels (ST), where a concrete pad foundation is anchored rigidly to the bedrock and was used as a base for two broadband Nanometrics Trillium Horizon 360 seismometers. Their self-noise is reported by the manufacturer in [17]. The two sensors were placed 40 cm apart and aligned towards the NS

Accepted Manuscript

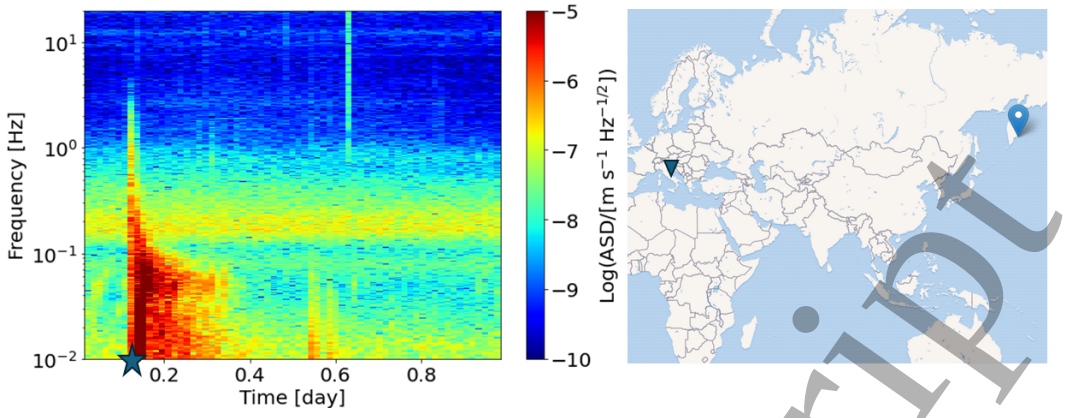


Figure 2: Spectrogram of the seismometer horizontal channel showing a teleseismic event observed during the first data acquisition at the ST measuring point. The M7.3 event occurred in the Kamchatka region (Russia), at a distance of approximately 8950 km from LNGS, on September 13, 2025 at 02:37:55 UTC. The effect in the low frequency band ($f < 0.1$ Hz) is clearly visible for several hours after the earthquake.

direction, protected with an insulating cover. The data from the two synchronized sensors were collected with a Nanometrics Centaur DAQ, powered with a buffer battery. Data were acquired in this measuring point from 8 September 2025 to 30 October 2025. The sensors were then moved to the other measuring point in the Hall C (HC) and installed on the hall floor close to the Borexino experiment water tank [15], acquiring data from 9 December 2025 to 14 January 2026. The two installations are shown in Figure 1. Specifics of sensors and DAQ used for the measurements are reported in Table 1.

Table 1: Seismometers and DAQ used in this work.

Type	**Model**	**Serial**	**Configuration**
Seismometer	Nanometrics Trillium Horizon 360	SN-003678	3.2×10^9 cnt m^{-1} s
Seismometer	Nanometrics Trillium Horizon 360	SN-003053	3.2×10^9 cnt m^{-1} s
DAQ	Nanometrics Cenatur CTR4-6S	SN-008458	10 V input range

2.2 Seismic noise measurements

A reliable estimate of the seismic background noise level requires measurements to be conducted by properly isolating the seismometers from spurious environmental effects, such as temperature fluctuations, convective currents, and vibroacoustic coupling. Furthermore, to correctly define the spectral amplitude, and specifically to derive an upper limit for the low-frequency tilt noise contribution (see the following Section 3), it is necessary to exclude high-energy transients, such as teleseismic events, from the analysis. Data selection and cleaning for the tilt extrapolation were performed through a rigorous manual inspection of the raw time-series. This visual approach was chosen to ensure the unambiguous identification of both local non-seismic glitches (e.g., anthropogenic, electronic or mechanical artifacts) and teleseismic events. Once a transient or an earthquake was identified, the corresponding time segment was removed from the analysis. To ensure that long-period instrumental ringing or residual low-frequency seismic tails were completely damped, a strict, event-specific veto protocol was implemented. For standard local glitches and anthropogenic transients, a safety margin of at least 15 minutes both before and after the event was discarded. Conversely, for major teleseismic events, such as the Kamchatka $M7.3$ earthquake shown in Figure 2, whose long-period effects can persist for several hours, the entire data segment preceding the earthquake shock was excluded, and a veto window of 4 hours was enforced immediately following the event to guarantee the complete decay of the primary seismic transients. This manual veto procedure allowed us to compute the Amplitude Spectral Densities (ASDs) exclusively on stationary, quiet background seismic periods, minimizing any statistical bias in the estimation of the median spectra. The subsequent ASD calculations were performed using 30 minutes-long time intervals with 50% overlap, ensuring a rigorous and fair comparison with the standard Peterson models [7] at the sub-microseismic frequencies.

Following the installation of the two broadband seismometers described in Section 2.1, we

Accepted Manuscript

calculated the Amplitude Spectral Densities (ASDs) using Welch's method [18], and the spectrograms of the seismic background noise for the horizontal and vertical components at measurement point 'ST'. To cross-check the ASD level obtained from the removal of energetic transients for the whole period used in Section 3, we calulated the ASD of a short-duration section of data without applying the transients removal, selecting a quiet period without strong transients. The ASDs and related spectrograms for the 'ST' point, calculated for the period from September 13 to September 15, 2025, are shown in Figure 3. Above 1 Hz, several lines produced by anthropogenic activities (e.g., laboratory work, active experiments, and ventilation) are clearly visible; some of these also exhibit a day/night pattern in the spectrograms. Below 1 Hz, typical microseismic peaks are apparent: the primary and secondary oceanic peaks at 80 mHz and approximately 200 mHz, respectively, and a peak at 750 mHz, related to semi-enclosed sea dynamics of the Mediterranean Sea.

These spectral features are produced by the continuous interaction of ocean waves with the seafloor and the coastline, generating compressible acoustic-gravity waves that propagate through the crust, creating a time-varying seismic background that is clearly detected even in the underground infrastructure of LNGS. The seismic ASD at the 'ST' point clearly follows the Peterson NLNM up to a few Hz, where it begins to be dominated by anthropogenic noise. At very low frequencies (i.e., between 10 and 100 mHz), the median falls within the NLNM-NHNM range [7], although it is slightly higher along the N-S axis. These ASDs differ from previous findings [13], which showed a significantly higher noise level exceeding the NHNM. This suggests that previous measurements were affected by instrumental artifacts, likely due to the sensors themselves or a lack of proper insulation. The slightly higher noise level along the N–S direction compared to the E–W direction in Figure 3 could be linked to the orientation of the sensors relative to the service tunnel, along which forced ventilation is usually present.

Given the 40 cm spatial separation between the two seismometers, any macroscopic low-frequency ground motion, either purely translational waves ($\lambda \gg 1$ km below 70 mHz) or genuine large-scale ground tilt is expected to be highly coherent. Consequently, the observed drop in the coherence function to a baseline level of $\sim$0.2 below 70 mHz (Figure 5) provides crucial physical insights. It is worth noting that a coherence value of ~ 0.2 corresponds to the statistical noise floor (bias) inherent to the coherence estimator when computed over a finite number of time segments, rather than indicating a genuine physical coupling. Therefore, this lack of significant coherence establishes that a dominant, common seismic tilt signal does not emerge above the instrumental noise floor. Instead, it demonstrates that the individual sensor records in this very-low frequency band are governed by independent instrumental self-noise or localized thermal fluctuations within the protective shielding. This statistical incoherence rules out a predominant common environmental tilt effect and justifies the interpretation of the extrapolated spectra below f_0 as a conservative upper bound rather than a direct measurement of ground tilt.

On December 9, 2025, we moved and installed the two seismometers on the floor of Hall C (site 'HC'), near the Borexino experiment infrastructure [15]. This site is inherently noisier than 'ST', as it is closer to the scientific equipment of experiments hosted in the hall. In particular, the nearby water tank of the Borexino experiment was empty and open during the measurements, showing a clear airflow through the whole structure. For the 'HC' point as well, we selected a quiet data sample without strong transients from the end-of-year holiday period (December 28-31), when no significant activities were underway in the underground laboratory. The ASDs and spectrograms from this data sample are shown in Figure 4. While the low-frequency features (i.e., microseisms and noise levels below 70 mHz) and the microseismic storm modulations are quite similar to those observed at the location 'ST', the anthropogenic noise above 1 Hz is higher, as expected due to the proximity to experimental equipment in the hall. In particular, all channels exhibit characteristic and largely persistent lines, which are likely linked to nearby experimental systems (e.g., pumps, cryostats, and electronics). In Figure 5 we also show the coherence between the horizontal channels for the same period at the 'HC' point: as in the previous measurement location, the low level of coherence drops to the same statistical noise floor, ruling out a predominant common rotational and/or translational noise. The relative increase of coherence below 20 mHz, with respect to the statistical noise floor, may be related to low-frequency resonances induced by the airflow through the Borexino empty water tank.

Accepted Manuscript

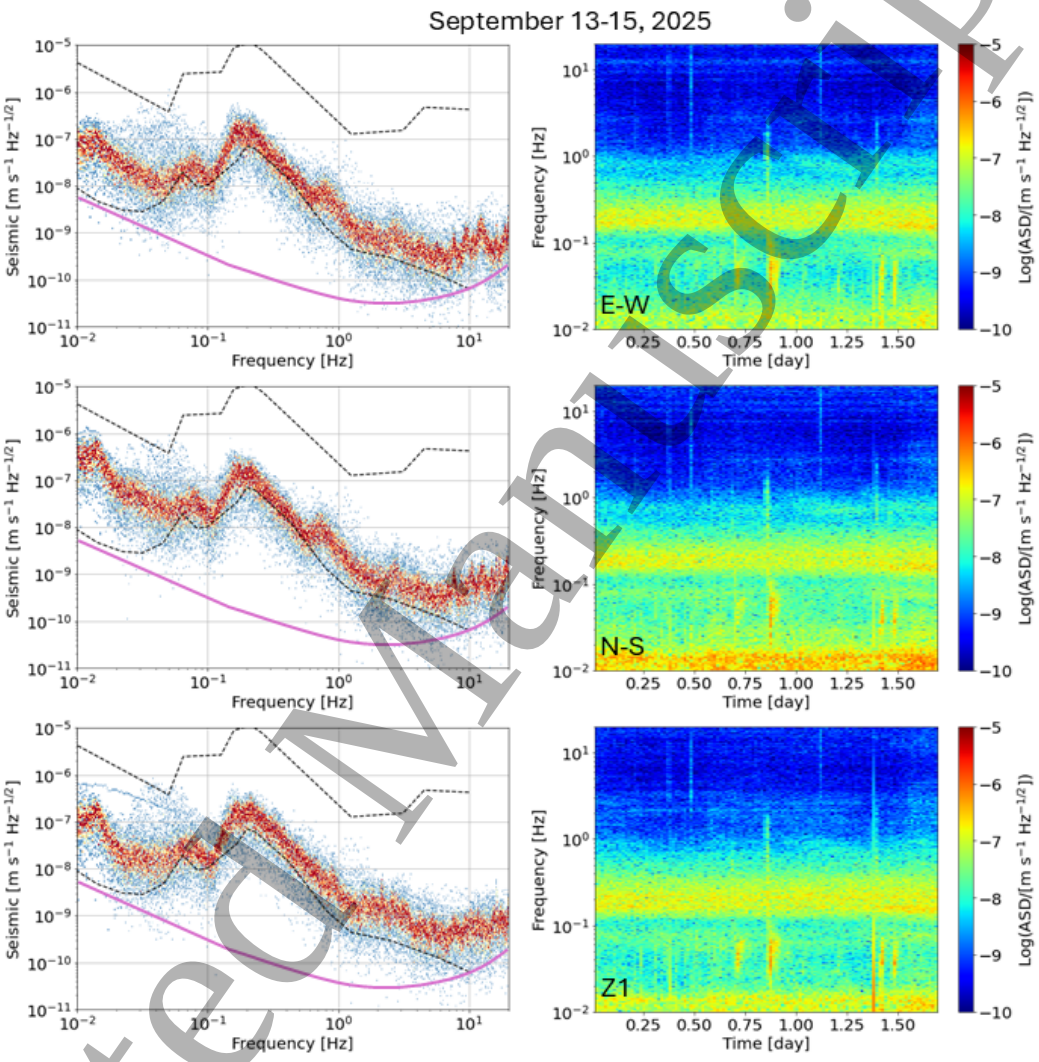


Figure 3: Probabilistic Amplitude Spectral Densities (PASD, left panels) and spectrograms (right panels) along E-W, N-S and vertical directions measured at the service tunnel (ST) point from September 13 to September 15, 2025. The purple line in PASD represents the nominal instrument self noise of the Trillium 360 Horizon seismometer[17], warm colors indicate a high probability of occurrence, highlighting the most frequent background noise levels (in red, the mode of the distribution), conversely, cold colors (e.g., dark blue) denote low probability, representing rare or transient events.

Accepted Manuscript

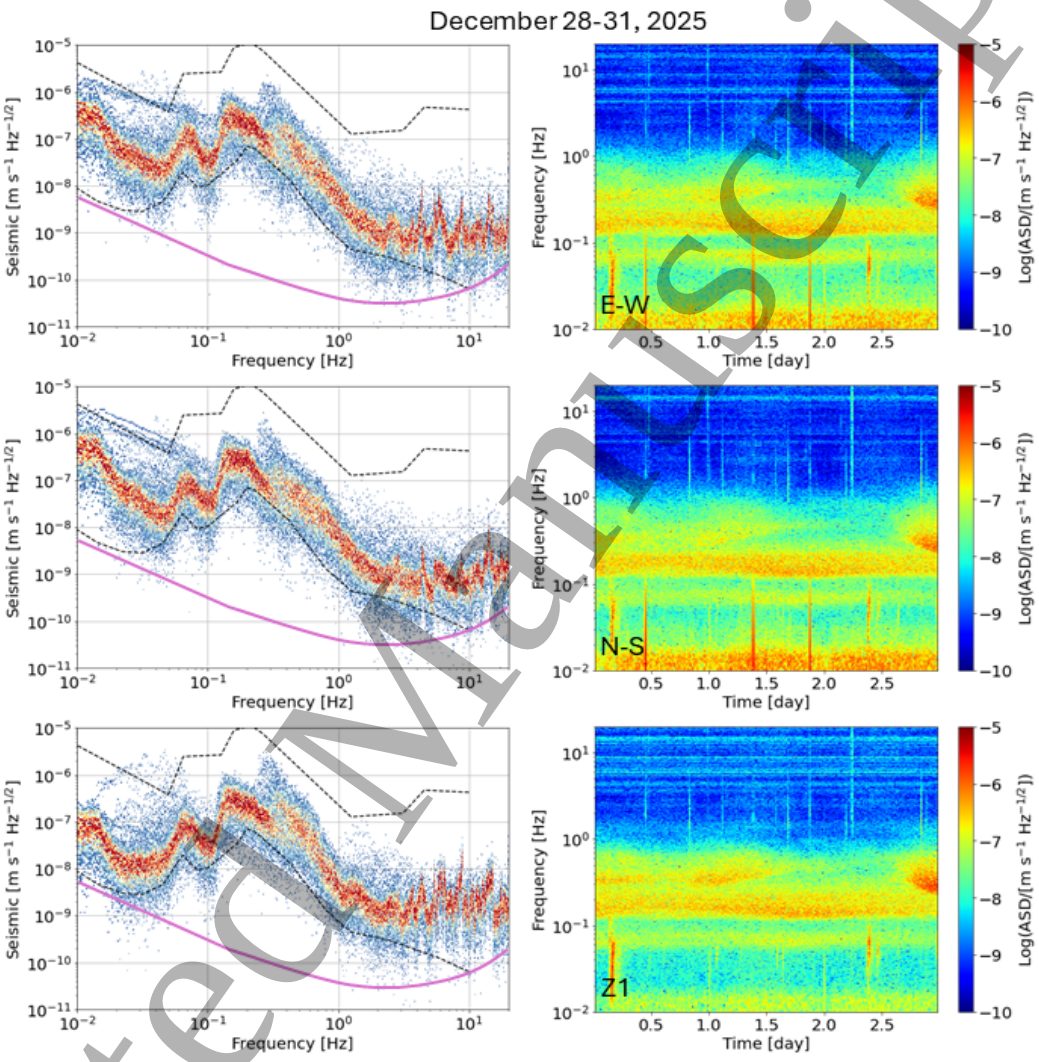


Figure 4: Probabilistic Amplitude Spectral Densities (PASD, left panels) and spectrograms (right panels) along E-W, N-S and vertical directions measured at the HC point (Hall C) from December 28 to December 31, 2025, during a period of low anthropic activity in the underground hall. The purple line in PASD represents the nominal instrument self noise of the Trillium 360 Horizon seismometer[17], warm colors indicate a high probability of occurrence, highlighting the most frequent background noise levels (in red, the mode of the distribution), conversely, cold colors (e.g., dark blue) denote low probability, representing rare or transient events.

Accepted Manuscript

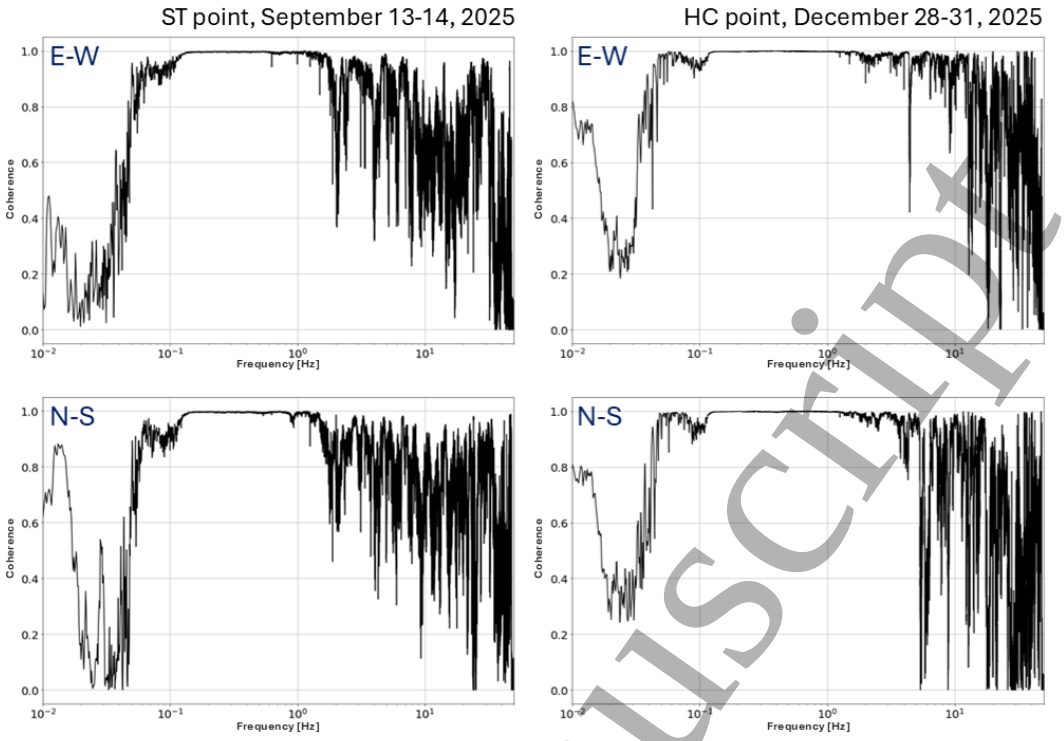


Figure 5: Coherence between the horizontal channels of the two seismometers at the ST measuring point (September 13-15, 2025) and at the HC measuring point (December 28-31, 2025). Coherences were calculated over continuous data segments for which no teleseisms or strong transients due to ongoing activities within the underground laboratories were present.

3 Ground tilt extrapolation

The development of instruments capable of directly measuring ground tilt in the frequency band from a few tens of mHz up to a few Hz remains one of the major scientific and technological challenges in geophysics [19]. Environmental conditions and local disturbances make this task extremely complex, and a universal direct solution has not yet been fully realized. Nevertheless, estimating ground rotation is achievable through indirect extrapolation methods applied to horizontal seismic data, which can be effectively used to establish a conservative upper limit.

3.1 Theoretical framework and extrapolation methodology

At low frequencies, horizontal seismic records are significantly contaminated by ground tilt due to gravitational cross-coupling, a phenomenon described by the Rodgers model [16]. For long-period surface waves and low-order spheroidal free oscillations, parametric effects are negligible, and the tilt response dominates the horizontal spectrum. Assuming a plane wave with phase velocity $c(f)$, the tilt spectrum $\theta(f)$ is directly related to the vertical displacement spectrum $W(f)$. The measured horizontal displacement $U_{\text{measured}}(f)$ is given by:

$$U_{\text{measured}}(f) = U(f) - i\frac{g}{2\pi f \cdot c(f)}W(f), \tag{1}$$

where $U(f)$ is the true horizontal translation and g is the gravitational acceleration. As $f \to 0$, the tilt-induced error diverges, effectively rendering the horizontal sensor an inclinometer. Conversely, the vertical component is immune to this direct linear coupling, providing a reference for pure vertical translation $W(f)$. This fundamental asymmetry enables the vertical record to serve as a coherent reference to isolate tilt-induced noise.

To establish an upper limit for ground rotation, we implement a multi-step methodology based on the spectral divergence of the channels:

1. We compute the amplitude spectral densities (ASDs) of the vertical and horizontal acceleration components ($\mathrm{m\,s^{-2}\ Hz^{-1/2}}$).

2. We identify an empirical frequency threshold ($f_0 < 100$ mHz) where the horizontal-to-vertical acceleration ASD ratio systematically reaches 1.70, ensuring the horizontal component is

Accepted Manuscript

dominated by non-translational effects. To capture the full dynamics of this separation, we track the signal divergence from the onset where the ratio exceeds 1.15. The interval between these landmarks defines the transition from coherent seismic translations to a regime dominated by instrumental self-noise, as evidenced by a concomitant decrease in inter-sensor coherence.

3. We interpret the uncorrected horizontal acceleration $a_h(f_0)$ at the threshold frequency as a conservative upper bound for tilt-induced acceleration, where $a_h(f_0) \approx g \cdot \theta(f_0)$.

While the instrument response to tilt is derived from the Rodgers framework [16], the low-frequency environmental ground rotation spectrum typically follows an empirical power-law trend. Specifically, the tilt acceleration spectrum exhibits an f^{-1} dependency, consistent with the long-period behavior of ambient atmospheric pressure fluctuations and temperature-induced gradients that drive local ground deformation. Although the Sorrells model [20] suggests that surface-generated atmospheric tilt decays rapidly at depth, it also implies that local ventilation or thermal micro-climates drive a similar f^{-1} acceleration baseline. Consequently, we extrapolate the ground rotation upper limit $\theta(f)$ as:

$$\theta(f) = \frac{a_h(f_0)}{g} \left(\frac{f_0}{f} \right), \tag{2}$$

where $\theta(f)$ is in rad $\mathrm{Hz}^{-1/2}$. We evaluate $g\theta(f)$ contribution to estimate ground tilt upper limits at the LNGS site, providing a direct comparison with data from the KAGRA facility.

3.2 LNGS tilt upper limit

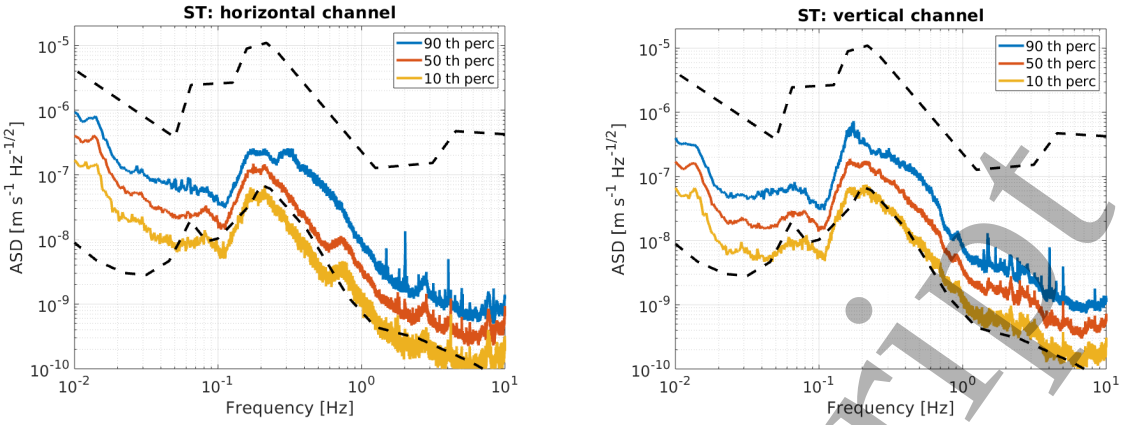
To estimate the upper limit of ground tilt at the LNGS site, we utilized data acquired during the seismic monitoring campaign detailed in Section 2.2.

3.2.1 ST station We computed the amplitude spectral density (ASD) percentiles for both horizontal and vertical channels during quiescent intervals from September 8 to September 18, 2025. Figure 6 presents the 50th percentile (median) spectral profiles for the horizontal and vertical degrees of freedom. The tilt-induced contribution was estimated by superimposing the vertical and horizontal median ASDs. We identified an empirical threshold $f_0 = 33$ mHz as the frequency at which the horizontal to vertical acceleration ratio reaches 1.70. By adopting the spectral amplitude $a_h(f_0)$ as a calibration point, we computed the ground rotation upper bound following Equation (2). By adopting the spectral amplitude $a_h(f_0)$ as a calibration point, we computed the ground rotation upper bound following Equation (2). To evaluate the stability of this selection for the ST station, a quantitative sensitivity analysis was performed by shifting the anchoring point across the local transition frequencies: 52 mHz ($H/V = 1.18$), 46 mHz ($H/V = 1.75$), 34 mHz ($H/V = 2.08$), and 11.2 mHz ($H/V = 2.40$). Evaluating the extrapolated spectrum shows that shifting f_0 to 52 mHz introduces an amplitude variation of a factor of 1.49 (+48.9%) relative to the nominal baseline threshold. At the lower boundary of 11.2 mHz, the extrapolated amplitude varies by a factor of 0.97 (−3.4%). This demonstrates that the final ground tilt spectrum for the ST station is tightly bounded between 0.97 and 1.49 times the nominal curve across the entire channel separation region. A similar stability analysis was performed for the other measurement sites, yielding fully consistent results; for the sake of brevity, these specific numerical values are omitted.

Figure 9(a) illustrates the vertical and horizontal acceleration profiles in conjunction with the "Extrapolated Tilt Upper Limit." This bound represents a conservative estimate constrained by the instrumental noise floor, rather than a direct measurement of coherent environmental ground rotation.

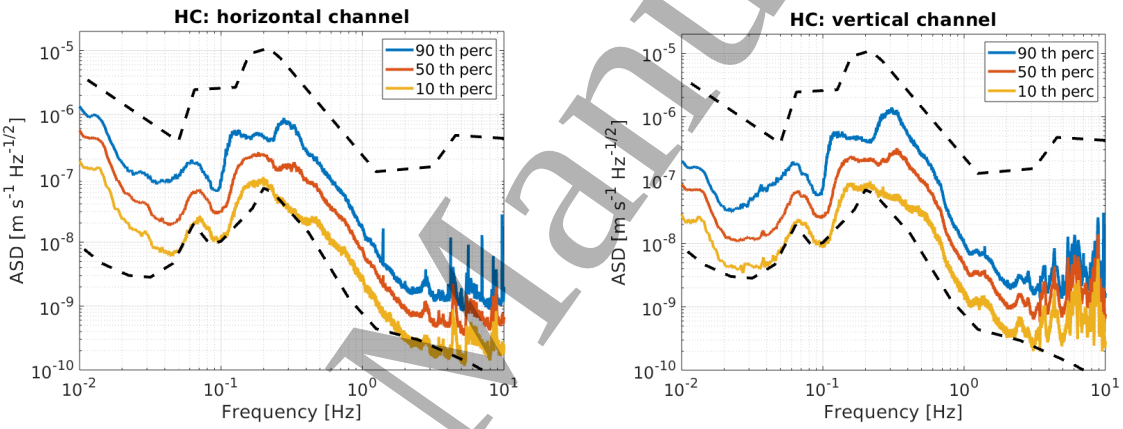
3.2.2 HC station We computed the spectral percentiles for the horizontal and vertical channels during the end-of-year holiday period, from December 21 to December 31, 2025. Figure 7 displays the percentiles of the seismic data for both degrees of freedom.To estimate the ground tilt, we superimposed the 50th percentile (median) curves of the vertical and horizontal components to identify the empirical threshold $f_0 = 37$ mHz, defined by the onset of systematic spectral divergence. Following the determination of the acceleration ASD value $a_h(f_0)$ at f_0, we extrapolated the ground rotation upper limit using Equation (2). Figure 9(b) shows the vertical and horizontal seismic profiles alongside the resulting ground tilt upper bound.

Accepted Manuscript



(a) (b)

Figure 6: Seismic noise percentiles for the Service Tunnel (ST) station, recorded by a Trillium 360s broadband seismometer. Panels (a) and (b) display the 10th, 50th (median), and 90th percentiles for the horizontal and vertical degrees of freedom, respectively. Amplitude spectral densities (ASDs) are given in m s^{-1} Hz$^{-1/2}$. The Peterson New Low Noise Model (NLNM) and New High Noise Model (NHNM) [7] are plotted for reference.



(a) (b)

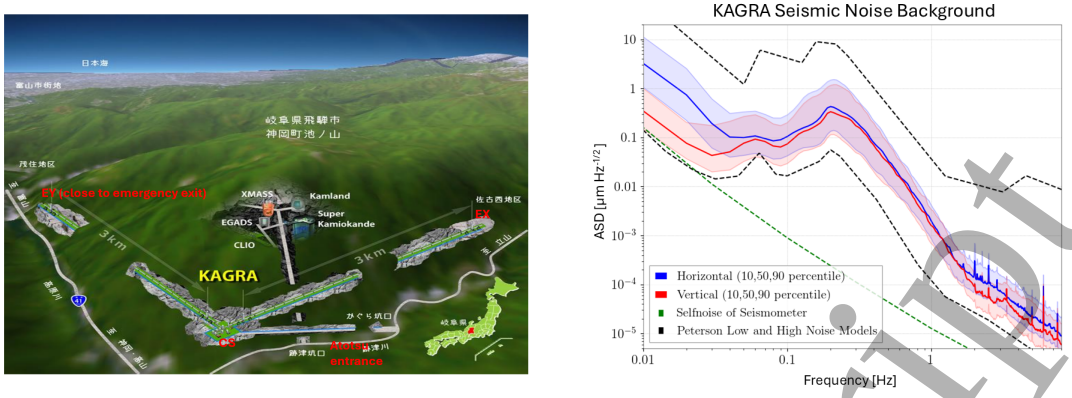
Figure 7: Seismic noise percentiles for the Hall C (HC) station, recorded by a Trillium 360s broadband seismometer. Panels (a) and (b) display the 10th, 50th (median), and 90th percentiles for the horizontal and vertical degrees of freedom, respectively. Amplitude spectral densities (ASDs) are given in m s^{-1} Hz$^{-1/2}$. The Peterson New Low Noise Model (NLNM) and New High Noise Model (NHNM) [7] are plotted for reference.

3.3 KAGRA tilt upper limit

To provide a benchmark for our site-characterization study, we compared our results with seismic data from the KAGRA gravitational-wave observatory (Kamioka, Japan) [21]. Located deep within a low-noise crystalline rock environment, the KAGRA detector represents a third-generation-like infrastructure that aligns closely with the environmental target specifications defined for the Einstein Telescope. The vertical and horizontal seismic percentile spectra were provided by the KAGRA Collaboration, recorded using Nanometrics Trillium 120 broadband seismometers installed at the X-end station. Following standard site-characterization protocols, the KAGRA Collaboration performed the initial data selection and quiet-period characterization. We utilized their median background profiles to apply our tilt-extrapolation methodology. Figure 8(b) displays the seismic percentiles for both degrees of freedom.

By superimposing the horizontal and vertical acceleration ASDs, we identified a site-specific empirical threshold of $f_0 = 30$ mHz. At this frequency, the horizontal spectrum diverges from the vertical translational profile by a ratio exceeding 1.70, signaling the transition where localized thermal fluctuations or instrumental self-noise dominate over coherent seismic translations. As shown in Figure 9(c), the horizontal acceleration spectral density $a_h(f_0)$ was utilized as the anchor

Accepted Manuscript



(a) (b)

Figure 8: The KAGRA observatory infrastructure and its seismic background. Panel (a) shows the Kamioka underground facility. Panel (b) displays the seismic noise percentiles (10th, 50th, and 90th) measured at the X-end station with a Nanometrics Trillium 120 broadband seismometer. Displacement spectral densities are given in μm Hz$^{-1/2}$, with the Peterson NLNM/NHNM [7] models converted to displacement for reference. Data in panel (b) were provided by the KAGRA Collaboration.

point for the ground rotation spectrum. Applying the model defined by Equation (2),assuming an f^{-1} power-law decay above f_0, we extrapolated the ground tilt noise upper limit. This profile provides a rigorous benchmark and confirms that under stringent underground shielding, the apparent low-frequency horizontal excess is bounded by instrumental noise, offering a quantitative baseline to evaluate the environmental tilt limits observed at the LNGS stations.

3.4 Comparison and impact on the ET-LF sensitivity

Once the seismic percentiles and tilt models for both sites were extrapolated, they were compared. With reference to Figure 9 panel (d), the tilt upper limit at LNGS is approximately 2 times higher than the extrapolated value for KAGRA . These results reflect the fundamentally different nature of the two laboratories. Kamioka hosts the KAGRA gravitational-wave detector, an infrastructure similar to what is planned for ET, and its seismic environment in the relevant frequency band is relatively quiet. In contrast, LNGS hosts a variety of experiments, including cosmic-ray, dark matter, and neutrino detectors, which employ instrumentation that could be inherently noisier in the frequency range relevant for gravitational-wave studies. As a final analysis, we evaluate whether our results are compatible with the Einstein Telescope low-frequency (ET-LF) target sensitivity [22], which officially extends down to 2 or 3 Hz [2]. Neglecting the contribution of control noises, which are well known to dominate the very low-frequency region ($f < 2$ Hz) and fall outside the scope of this work, we establish the baseline impact of the extrapolated tilt levels when filtered through the open-loop cross-coupling transfer function ($T_{x-\theta}$) of a 12-m-tall seismic isolation system designed for ET-LF [23]. Crucially, as shown in Figure 10, when the extrapolated limit on the tilt noise, filtered through a 12-m-tall Super Attenuator (SA), is superimposed onto the official Einstein Telescope design requirements, even our conservative upper bounds at LNGS comply with the suspension active seismic isolation targets.

Overall, this comparative assessment demonstrates that while both underground facilities provide highly stable baselines for precision physics, their site-specific seismic profiles are somehow shaped by institutional utility and local specific instrumentation. The Kamioka infrastructure, engineered specifically to host the KAGRA gravitational-wave observatory, maintains a remarkably quiet ambient baseline within the primary gravitational-wave detection band. Conversely, the multi-disciplinary experimental layout at LNGS exposes the site to higher anthropic seismic noise levels, resulting in a slightly higher upper limit on the extrapolated ground tilt below 70 mHz driven by nearby experimental machinery. Nevertheless, our projection framework underscores that this elevated environmental background does not preclude its suitability; when filtered through the 12-m-tall Super Attenuator transfer function, the LNGS tilt upper bounds remain compliant with the ET-LF targets. These empirical criteria confirm the technical feasibility of managing site-specific ambient noise, offering crucial guidance for the engineering and optimization of next-generation gravitational-wave detectors.

Accepted Manuscript

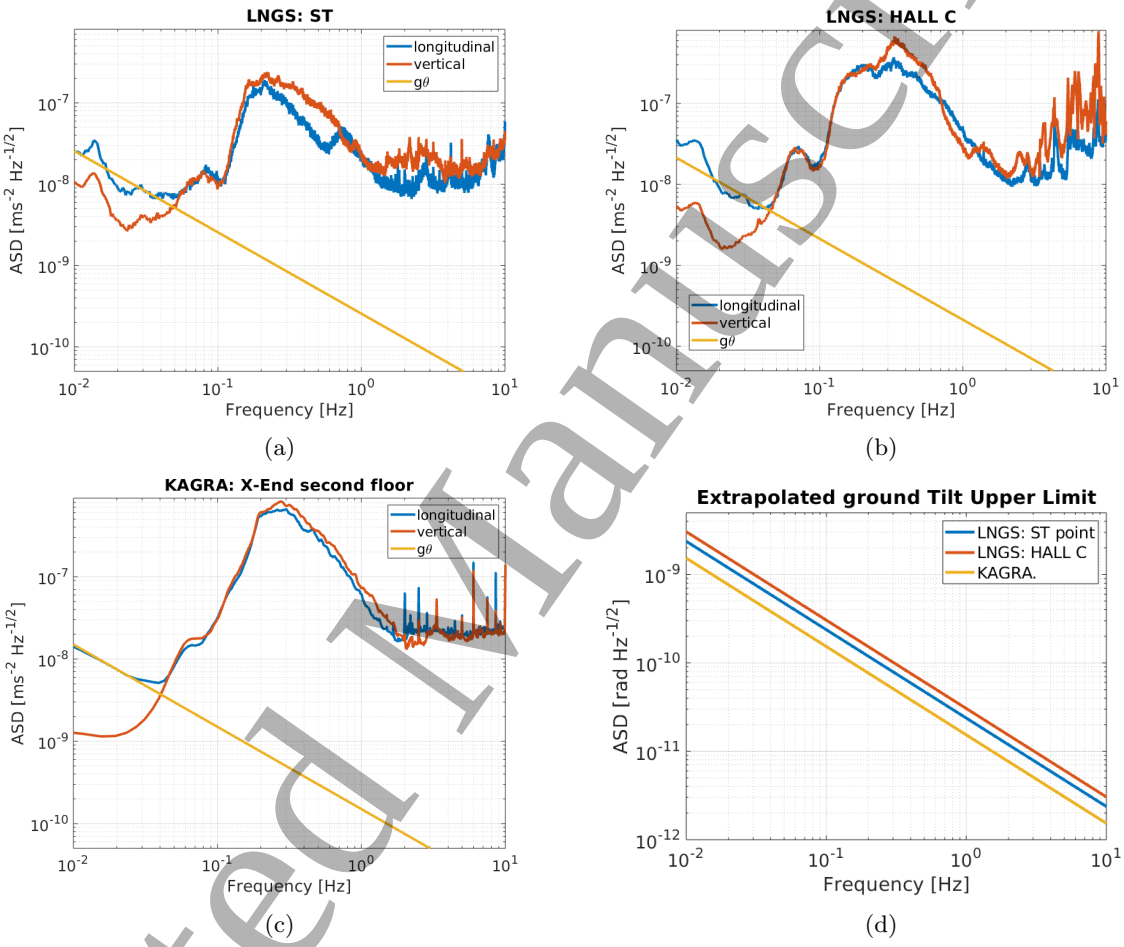


Figure 9: Extrapolated ground tilt noise limits. Panels (a), (b), and (c) display the tilt extrapolation models derived from the 50th-percentile (median) seismic noise spectra at the LNGS ST station, the LNGS HC station, and the KAGRA site, respectively. Panel (d) provides a comprehensive comparison of the resulting ground tilt noise upper limits across the three analyzed environments.

Accepted Manuscript

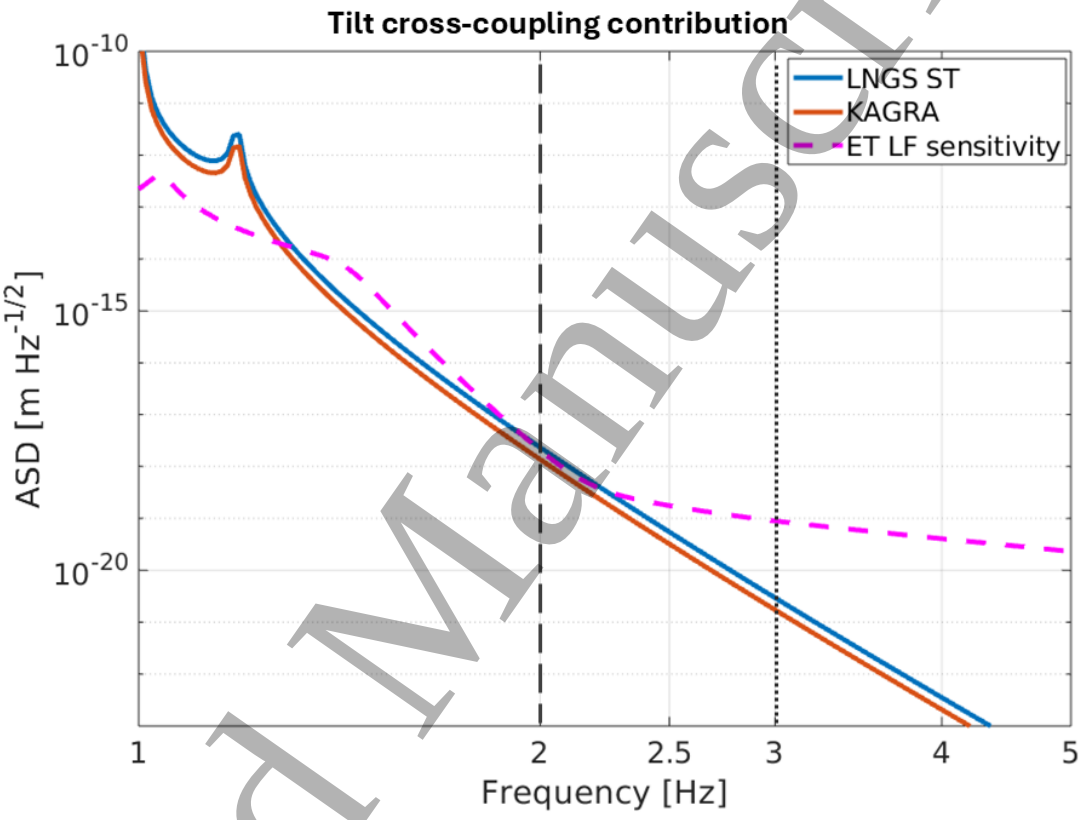


Figure 10: Comparison between the extrapolated ground tilt noise upper limits, filtered through a 12 m tall Super Attenuator (SA), and the Einstein Telescope (ET) low-frequency target sensitivity. The plot superimposes the conservative tilt upper bounds derived for the LNGS Service Tunnel (ST, blue curve) and KAGRA (red curve) sites, expressed in m $\mathrm{Hz}^{-1/2}$, after projection onto the longitudinal displacement via the open-loop cross-coupling transfer function ($T_{x-\theta}$) of the SA configuration [23], against the official ET-LF sensitivity [22] (dashed purple line). The vertical dashed and dotted grey lines represent respectively the proposed lower frequency of the ET-LF detection band at 2 and 3 Hz.

Accepted Manuscript

4 Discussion and Conclusions

In this work, we investigated the low-frequency seismic background noise in an underground scientific facility. We started from the Laboratori Nazionali del Gran Sasso (LNGS) underground laboratory, following previous findings of excess noise at very low frequencies (i.e., below 70 mHz) at this site, which were tentatively interpreted as potential ground tilt noise.

We crosschecked these previous measurements by deploying two broadband seismometers, properly insulated and aligned, at two separate locations: first in a quieter location, a service tunnel (ST), then in the experimental Hall C (HC). Our results show significantly lower noise levels below 70 mHz compared to previous studies, falling well within the Peterson NLNM-NHNM bounds [7].

Rather than relying on qualitative assessments, the strict lack of significant statistical coherence (~ 0.2) observed between the adjacent horizontal channels below 70 mHz allows us to quantitatively reject the hypothesis of a dominant common environmental seismic or tilt background emerging above the instrumental noise floor. Instead, this baseline coherence matches the statistical estimator bias for uncorrelated signals, proving that the low frequency horizontal spectra are mutually limited by independent instrument self-noise or localized thermal fluctuations within the protective shielding. Previous findings of excess noise below 70 mHz can be then explained as result of systematic effects, such as sub-optimal environmental insulation of the seismometer and sensor self-noise.

Consequently, we established conservative, quantitative upper limits on the ground tilt noise spectrum using an extrapolation framework based on Rodgers [16]. The derived tilt upper limits at LNGS range between approximately 3×10^{-9} rad Hz$^{-1/2}$ and 3×10^{-12} rad Hz$^{-1/2}$ in the 10 mHz-10 Hz band, with the Service Tunnel showing a factor of 1.5 lower noise compared to Hall C due to its physical isolation from active experimental facility infrastructure (such as cryogenic and vacuum systems running 24/7).

Finally, we compared our results with data obtained from the KAGRA site in Kamioka, Japan. Given the operational and technical similarities between KAGRA and the Einstein Telescope (ET), we consider the underground environment of KAGRA a valuable benchmark, even though the ET infrastructure and site geophysical features will be different. The tilt upper limit at LNGS is approximately two times higher than the extrapolated upper limit for KAGRA, reflecting the different nature and density of experimental instrumentation hosted in the two infrastructures. Specifically, projecting these conservative LNGS upper bounds through the transfer function of a 12-m-tall Super Attenuator (SA) demonstrates that the residual tilt-induced noise remains strictly compliant with the official ET low-frequency suspension isolation requirements. This verification provides vital engineering guidance for the development of active tilt-attenuation controls for the future ET observatory, confirming that underground ambient tilt noise is manageable within current sensor-fusion design paradigms, ensuring that active controls can suppress the residual noise without saturating the actuators or compromising the target low-frequency sensitivity of the future ET observatory.

Acknowledgments

The authors acknowledge the Laboratori Nazionali del Gran Sasso for allowing the measurement campaign in the underground laboratory, and the KAGRA Collaboration for providing seismic data measured at the Kamioka site. This work has been supported by the INFN with the agreement *Protocollo di Intesa tra Ministero dell'Istruzione, dell'Università e della Ricerca, la Regione Autonoma della Sardegna, l'Istituto Nazionale di Fisica Nucleare e l'Università degli Studi di Sassari finalizzato a sostenere la candidatura italiana a ospitare l'infrastruttura Einstein Telescope in Sardegna e al potenziamento di Virgo.*

Data availability statement

This manuscript has associated data stored in a data repository, available upon request (please contact the corresponding author).

Accepted Manuscript

References

[1] Punturo M., et al., 2010. The Einstein Telescope: a third-generation gravitational wave observatory, *Class. Quantum Grav.* **27** 194002.

[2] ET Steering Committee Editorial Team, 2020. *ET design report update 2020*, ET-0007A-20 (public), https://apps.et-gw.eu/tds/?content=3&r=17245

[3] Accadia T., et al., 2011. The seismic Superattenuators of the Virgo gravitational waves interferometer, *Low Freq.Noise Vibrat.Act.Control* **30**, 1 63–79

[4] Longuet-Higgins M.S., 1950. A theory of the origin of microseisms, *Philos. Trans. R. Soc. London* **243** 1–35.

[5] Cessaro R.K., 1994. Sources of Primary and Secondary microseisms, *Bull. Seismol. Soc. Am.* **84** No.1 142–148.

[6] Zürn W., et al., 2022. Modelling tilt noise caused by atmospheric processes at long periods for several horizontal seismometers at BFO –a reprise, *Geophysical Journal International* **228**, 2, 927–943.

[7] Peterson J., 1993. Observation and modeling of seismic background noise, *U.S. Geol. Surv. Open-File Rept.* **2** 93-322.

[8] Naticchioni L., et al., 2014. Microseismic studies of an underground site for a new interferometric gravitational wave detector, *Class. Quantum Grav.* **31** 105016.

[9] Naticchioni L., et al., 2020. Characterization of the Sos Enattos site for the Einstein Telescope, *J. Phys.: Conf. Ser.* **1468** 012242.

[10] Di Giovanni M., et al., 2021. A Seismological Study of the Sos Enattos Area—the Sardinia Candidate Site for the Einstein Telescope, *Seismological Research Letters* **92 (1)** 352–364.

[11] Di Giovanni M., et al., 2023. Temporal variations of the ambient seismic field at the Sardinia candidate site of the Einstein Telescope, *Geophysical Journal International* **234 (3)** 1943–1964.

[12] Naticchioni L., et al., 2023. Characterizing the Sardinia candidate site for the Einstein Telescope, *PoS Proc. Sci.* **441** 012242.

[13] Belfi J., et al., 2016. Ginger/G-Gran Sasso-RD Annual Report 2015, in *Annual Report 2015 - Laboratori Nazionali del Gran Sasso*, 104-130.

[14] Andric, T., Harms, J., Caravella, I. et al., 2026. Gemini: the first underground testbed for seismic isolation and inter-platform control in next-generation gravitational-wave detectors., *Eur. Phys. J. Plus* **141**, 170.

[15] Alimonti G., et al., 2009. The Borexino detector at the Laboratori Nazionali del Gran Sasso, *Nucl.Instrum.Meth.A 600* **600** 568–593.

[16] Rodgers P. W., 1968. The response of the horizontal pendulum seismometer to Rayleigh and Love waves, tilt, and free oscillations of the earth, *Bulletin of the Seismological Society of America*, 58, 5.

[17] https://nanometrics.ca/instrumentation/products/seismometers/trillium-horizon-360

[18] Welch P. D., 1967. The Use of Fast Fourier Transform for the Estimation of Power Spectra: A Method Based on Time Averaging over Short, Modified Periodograms, *IEEE Transactions on Audio Electroacoustics*, AU-15, 70–73.

[19] Allocca A. et al. 2021. Picoradiant tiltmeter and direct ground tilt measurements at the Sos Enattos site, *Eur. Phys. J.*, 136, 1069.

[20] G. G. Sorrells, 1971. A preliminary investigation into the relationship between long-period seismic noise and local fluctuations in the atmospheric pressure field, *Geophys. J. Int.*, vol. 26, no. 1-4, pp. 71–82.

[21] Akutsu T., et al., 2019. First cryogenic test operation of underground km-scale gravitational-wave observatory KAGRA, *Class. Quantum Grav.* **36** 165008.

Accepted Manuscript

[22] Einstein Telescope Collaboration, ET-NoiseBudget: Interferometer Noise Budget and Sensitivity Models, Einstein Telescope Instrument Science Board (ISB), GitLab repository, URL: https://gitlab.et-gw.eu/et/isb/interferometer/ET-NoiseBudget.

[23] F. R. Spada, G. Losurdo, L. Lucchesi, M. Pinto, P. Ruggi, and L. Trozzo, 2026. Feasibility and Compliance Study for the Seismic Isolator of Low-Frequency Einstein Telescope Test Masses, *Journal of Physics: Conference Series*, vol. 3177, no. 1, p. 012097.

Accepted Manuscript